Rev. Adv. Mater. Sci. 46 (2016) 70-85

ASSESSMENT OF VARIOUS PROPERTIES EVOLVED DURING GRAIN REFINEMENT THROUGH MULTI-DIRECTIONAL FORGING

Rahul Gupta[1], Sanjay K. Panthi[2] and Sanjay Srivastava[1]

[1]Department of Material Science and Metallurgical Engineering, MANIT Bhopal 462003, India
[2]Advance Materials and Processes Research Institute, Bhopal 462024, India

Received: April 26, 2016

Abstract. The current article presents our approach toward the area of generation of various properties in different materials by grain refinement and also discusses different mechanism of strengthening through multi-directional forging (MDF) process (a severe plastic deformation process). During last decades, the researches in the field of multi-directional forging are growing enormously, which is making MDF, an interesting process to alter various properties of the materials along with its microstructure refinement. The modification of the various different properties of materials makes multi-directional forging process versatile, in terms of increasing processed materials applications. The present review of various literature based on different materials processed by MDF of the published data is an approach to bring in attention towards the usefulness of the process, increase of knowledge about various changed materials properties via MDF and to relate various different published results in terms of processing conditions, materials used, strain applied, and grain refinement.

1. INTRODUCTION

The division of grains into multiple numbers can be establish as a major microstructural feature affecting almost all mechanical and physical performance of the polycrystalline metals along with its biochemical and chemical behaviours. The organization of the grain structure with reduced size, recognize the materials with required properties. As the changes in various properties of the material are resulted with the decrease in grain size, the competition to introduce superior executing materials is also increasing day to day. The potential opportunity for materials microstructural refinement is the application of severe plastic deformation process (SPD). During previous era, SPD is scientifically as well as technically developed by P.W. Bridgman by applying the arrangement of large hydrostatic pressure and shear deformation for the processed materials [1,2]. Bridgman explains the general principle of SPD processes, which is presently widely accepted and readily being used for various different materials.

In last decade, the fabrication of bulk nano-structured materials using severe plastic deformation process has grown considerably with the aim of building novel functional and mechanical properties in the materials [3]. Processing through SPD refers various different metal forming experimental processes that can apply extremely high strains on materials and introduce newly refined ultrafine grain (UFG) structure, thereby introducing the changes in various properties of the materials. The main characteristic of SPD processing during the application of high strain is that the overall measurements of the specimen are maintained with the use of particular geometries such as designed dies, which

Corresponding author: R. Gupta; e-mail: rahulgupta087@gmail.com

© 2016 Advanced Study Center Co. Ltd.

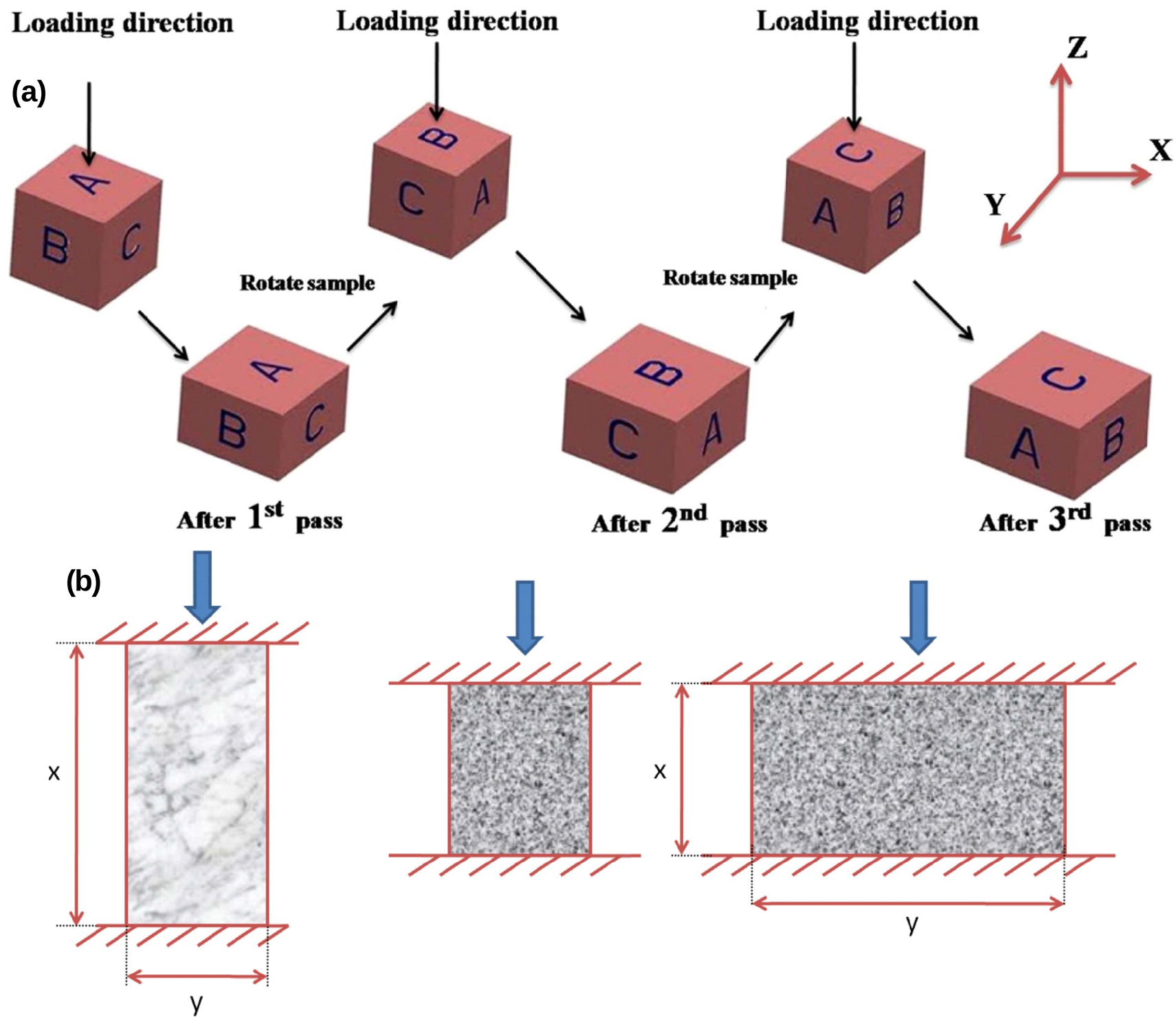

Fig. 1. (a) and (b) Schematic representation of MDF processing, reprinted with permission from Y. Estrin and A Vinogradov // Acta mater. **61** (2013) 782, (c) Elsevier 1999, and R. Gupta, S. Srivastava, N. K. Kumar and S. K. Panthi // Mater. Sci. Engg. A **654** (2016) 282, (c) Elsevier 1999.

averts free flow of materials and thus generate considerable hydrostatic pressure which increases the dislocation density in material and refines grain exceptionally [4].

The principal SPD methods for the production of ultrafine grained structure in various materials by applying large plastic strain are [5-8], (a) Multi-directional forging (MDF), (b) Equal channel angular pressing (ECAP), (c) High pressure torsion (HPT), (d) Accumulative roll bonding (ARB), and (e) Twist extrusion (TE).

(a) Multi-directional forging (MDF)

MDF is introduced for first time during 1990 through the development of ultrafine grained structure in bulk billets [9,10]. MDF is a recurrence of free forging process numerous times with the alterations of axes of loading including setting and pulling operations as shown in Fig. 1a [11]. The MDF processing is usually applied in the temperature period of 0.1 to 0.5 of the absolute melting temperature of materials, so the grain refinement is associated with dynamic recrystallization during MDF. The strain homogeneity fabricated by MDF process is lesser than produced during ECAP and HPT processes. On the other hand, MDF can be used to produce ultrafine grained structure up to nano scale in brittle materials also, owing to processing at elevated temperatures and comparatively lower specific load involved on tooling. Furthermore, the proper selection of strain rate-temperature system of deformation directs to required grain refinement during MDF [11]. MDF is demonstrated as an effective process for the production of large size billets with ultrafine grained structures and successfully applied to various materials [12].

The non-uniform equivalent strain during MDF is calculated by using Eq. (1) [13]

$$\in_{eff} = N \frac{2}{\sqrt{3}} \ln\left(\frac{x}{y}\right), \quad (1)$$

where, x and y are the dimensions of specimen as shown in Fig. 1b, N is the number of processing steps.

T. Sakai et al. [14] enlisted the advantages of MDF for metallic materials. (i) MDF can be applied by using conventional forging machine for large scale production without any need of special machine tools. (ii) The analysis and investigation of microstructure developed during MDF and the stress vs. strain relation can be studied analytically. (iii) The mechanisms of formation of microstructure during deformation and the relationship between them can be presented specifically.

Among various SPD procedures, the MDF process is an emerging method of SPD, because of above listed advantages and its ability to produce grain structure up to ultrafine (100-1000 nm) and nano scales (< 100 nm) for different materials enlisted in Table 1. The materials processed by SPD process with such a grain scale generally termed as nanoSPD materials [8]. MDF is also works on the same principle of conveying a very large plastic strain to a specimens, which requires substantial investments in MDF die design and its fabrication, because as per the applications of MDF the die is required to withstand very high material forming repeating loads and should not caused any smash up to the working materials as well. The good designed tooling used during MDF could results no significant cross sectional dimension change of the workpiece materials due to constrained material free flow during deformations, and easy application of high hydrostatic pressure.

Table1. Tabulation of different materials processed, strain applied, refined grains and properties evolved during MDF.

Ref.	Processing	Materials	Equivalent strain	Grain size/ crystallite size	Mechanical properties (yield strength (Y.S), Ultimate tensile strength (UTS), Hardness (Hv)), and others
[14]	MDF at low and high temperature	Pure Cu and Al alloy	18 and 1.2	For Cu around 150 nm	For Cu Max. flow stress - around 440 MPa
[22]	MDF at 298K and 418K	Cu	4 and 8	0.30 μm and 0.28 μm after 4 and 8 strains	At 298K around (Max. flow stress - 450 MPa), At 418K around (Max. flow stress - 340 MPa)
[23]	MDF at RT	Cu and Al-Cu	7 and 2.5	For Cu - 21.84 nm and Al-Cu 20-25 μm	For Cu, (Max. flow stress - 640 MPa and Hardness -177 Hv), For Al-Cu, (Max. flow stress - 375 MPa and Hardness – 110 Hv)
[24]	MDF at RT	Cu alloy (high leaded tin bronze)	0.75	90 nm	Y.S - 185 MPa, U.T.S - 346 MPa, Hardness - 175 ± 2 Hv, Ductility - 6.39 %, Dislocation density - 1.52 x 10^{15} m^{-2}
[25]	MDF at RT	Oxygen free Copper (99.99%)	7.8	378 nm sub-grains	Saturated stress - 400 MPa
[26]	MDF, TE, ECAP, and HPT at RT (room temperature)	Oxygen free Copper (99.98%)	50 during MDF	225 nm via MDF	Hardness - around 1.12 GPa at 300K, Dislocation density - 7 ± 1 x 10^{14} m^{-2}
[27]	MDF at 300K	Pure Cu	6	< 1 μm	U.T.S - around 350 MPa, Hardness - around 1300 Hv/ MPa
[28]	MDF at RT and ageing	AZ61 Mg alloy	2.5	0.6 μm	Y.S - 500 MPa, U.T.S - 540 MPa, Ductility – 4%
[29]	MDF at multi-temperatures	AZ61 Mg alloy	4.158	8 μm	Y.S - 300 MPa, U.T.S - 199 MPa, Ductility - 19%, Hardness - 72 Hv

[39]	MDF under decreasing temperature between 623-503 K followed by rolling	AZ61 Mg alloy	4	0.8 μm	U.T.S - 440 MPaDuctility - 20%
[31]	MDF under decreasing temperature between 643-483K followed by cold rolling	AZ61 Mg alloy	4	Around 1 μm	True stress - around 100 MPa at 503K, Ductility - 20 %, Hardness - 99 Hv
[32]	MDF at RT	AZ61 Mg alloy	2	0.6 μm	Y.S - 480 MPa, U.T.S - 525 MPa, Ductility - 5%
[33]	MDF at 500 °C to 400 °C, precede by hot rolling and annealing	Mg-Gd-Zn alloy	4 during MDF	12 μm	Y.S - 143 MPa, U.T.S - 223 MPa, Ductility - 40.9%
[34]	MDF at RT followed by various annealing	AZ21 Mg alloy	1.5	3.8 μm	UTS - around 350 MPa, Hardness - around 92 Hv
[35]	MDF at 473K	AZ31 Mg alloy	1.5	-	True stress - around 235 MPa
[36]	MDF under decreasing temperature between 623-423K	AZ31 Mg alloy	4.8	0.36 μm	At low strain rate (Max. flow stress - 120 MPa), At high strain rate (Max. flow stress - 90 MPa).
[37]	Cold MDF followed by annealing	AZ31 Mg alloy	1.5	Around 9.5 μm	True stress - around 345 MPa
[38]	Cold MDF followed by annealing	AZ31 Mg alloy	5	1 μm	True stress - around 370 MPa, Hardness - around 990 Hv/ MPa
[39]	Hot MDF	AZ80 Mg alloy	3.2	< 2 μm	-
[40]	MDF under decreasing temperature between 623-403K	AZ31 Mg alloy	5.6	0.23 μm	Y.S - 400 MPa, U.T.S - 526 MPa, Ductility - 13% (All above values for 0.36 mm grain size)
[41]	MDF under decreasing temperature between 623-423K	AZ31 Mg alloy	5	0.36 μm	True stress - around 145 MPa, Hardness - around 1010 Hv/ MPa
[42]	MDF at different temperature (370 °C to 450 °C)	Particulate reinforced Mg metal matrix composite	6 MDF pass	Around 5.5 μm	Y.S - around 280 MPa, U.T.S - around 315 MPa, Ductility - 1.16%
[43]	MDF at 420 °C	Particulate reinforced Mg metal matrix composite	6 MDF pass	Around 10 μm after 1 pass	Y.S - around 175 MPa, U.T.S - around 220 MPa, Ductility - 1.6%
[44]	MDF and partial remelting route	ZK60 Mg alloy	2.1	-	Thixoformed at 560 °C (Y.S - 178 MPa, U.T.S - 290 MPa, Ductility - 8%) Thixoformed at 574 °C (Y.S - 202 MPa, U.T.S - 315 MPa, Ductility - 13%)
[45]	MDF at 130 °C	6061 Al alloy	-	-	U.T.S - 385.7 MPa, Ductility - 11.17%
[46]	MDF at liquid nitrogen temperature	Al 6061 alloy	5.4	250 nm	Y.S - 380 MPa, U.T.S - 388 MPa, Ductility - 4.5%, Hardness - 115 Hv
[47]	MDF at 490 °C	7475 Al alloy	6	7.5 μm	-

[48]	MDF at 763K with different strain rates	7475 Al alloy	6.3	5.5 and 7.5 μm	True stress - around 42 MPa and 32 MPa
[49]	MDF at 573 to 763K	7475 Al alloy	7	6 μm	Max. flow stress - around 70 MPa
[50]	MDF at RT	AA3104 Al alloy	3.56	0.37 μm	Y.S - 330 MPa, U.T.S - 300 MPa
[51]	MDF at RT	AA1100 Al alloy	6.4	80-200 nm	Y.S - 264 MPa, Hardness - 80 Hv
[52]	MDF at RT and at 100, 300, 400 °C	AA3103 Al alloy	3	-	-
[53]	MDF	A356 Al alloy	1.4	-	Y.S - 173 MPa, U.T.S - 206 MPa, Hardness - 83.6 Hv
[54]	MDF at RT followed by non isothermal annealing	hot-extruded AA5056-H38 aluminum alloy	1.2	0.18 μm	Y.S - 152 MPa, U.T.S - 198 MPa, Electrical conductivity is decreased from 29 to about 25 IACS %.
[57]	MDF at 77K and 300K	Austenitic stainless steel (SUS 316)	6	5-10 nm	U.T.S – 2.1 GPa, Ductility - 20%, Hardness – 5 GPa
[58]	MDF at 500 °C and 800 °C	Austenitic stainless steel (304 type)	4	0.22 μm at 500 °C and 0.69 μm at 800 °C	Max. flow stress - about 800 MPa
[59]	MDF at RT	Low carbon steel	2.8	0.12 μm	Y.S - 850 MPa, U.T.S - 1115 MPa, Ductility - 7.1%, Hardness - around 260 Hv
[61]	MDF after preheated at 550 °C for 45 min.	HSLA steel	3.6	-	Y.S - 814 MPa, U.T.S - 817 MPa, Ductility – 14.62%, Hardness - 256 ± 3 Hv, Tensile test toughness (J) – 7.78, Slurry erosion rate - 1.11 x 10^{-3} $mm^3/h\ mm^2$
[62]	MDF after preheated at 500 °C for 50 min.	AISI 1016 steel	7.2	0.6 μm	U.T.S - 695 MPa, Ductility - 10%, Hardness - 277 Hv
[63]	MDF after preheated at 500 °C and holding for 50 min.	HSLA steel	3.6	0.6 μm	Y.S - 380 MPa, U.T.S - 813 ± 25.2 MPa, Ductility - 12.5 ± 0.2%, Hardness – 274.9 ± 9.2 Hv
[64]	MDF at 500 °C	Plain low carbon steel	1.3	0.5 μm	Y.S - 409 ± 23.3 MPa, U.T.S - 791 ± 7.2 MPa, Ductility - 12.08 ± 2.43%, Hardness - 253 ± 7.5 Hv
[66]	MDF at 600 °C	316 L stainless steel	4.2	0.86 μm	U.T.S - 1000 ± 65 MPa, Ductility - 14%, Hardness - 334 Hv, Improved localized corrosion resistance and sliding wear resistance
[68]	MDF at 500 °C	AISI 1024 steel	3.6	0.5 μm	U.T.S - 800 MPa, Ductility - 12%, Hardness - 253 Hv, Wear resistance is not improved
[69]	MDF at 973K in air	AISI201 stainless steel	1.2	5 μm	True yield stress - around 800 MPa, True ultimate stress - around 830 MPa

[70]	MDF at temperature between 500 °C and 700 °C	S304H austenitic stainless steel	3.5	0.1 μm	At 500 °C, (U.T.S - 810 MPa) At 700 °C, (U.T.S - 490 MPa)
[71]	MDF at close to -190 ℃	CP Titanium	1.18	100-200 nm	Y.S - 570 MPa, U.T.S - 840 MPa, Ductility - 12%
[72]	MDF followed by rolling at room temperature	Beta Titanium	5.4	1 μm	Elastic modulus - 60-65 GPa, U.T.S - 1100 MPa, Ductility - above 10%

(b) Equal channel angular pressing (ECAP)

Out of all SPD process, ECAP is the most developed technique. In ECAP, specimen as a rod shaped billet is pressed inside a die restricted by a channel which is bent at a sudden angle and shear strain is applied by passing the specimen through the intersecting point of two channel parts as shown in Fig. 2. The high strain can be applied to the specimen by repeating the process inside a die, as the billet cross sectional dimensions remains unchanged during the process. The continuous pressing cycle during ECAP leads to increase dislocation density in a billet along with UFG structure due to the accumulation of shear strain. There are numerous of modification in traditional ECAP are resulting day to day making ECAP to efficiently produce UFG structure, for e.g. introduction of back pressure [4,15,16].

(c) High pressure torsion (HPT)

In HPT, thin disk specimen is applied with torsional straining under high pressure usually in GPa range as shown in Fig. 3. During HPT, the specimen in a form of disk is placed within a die cavity, then the high hydrostatic pressure with the rotation of one anvil is applied that results plastic torsional straining. The small disk shaped specimen of usually 10-15 mm diameter and 1 mm thickness can be deformed by using HPT, which forms attractive products like bulk nano-magnets, arterial stunts, and devices of micro-electromechanical applications. Many attempts for making HPT to process larger bulk specimens are made during various studies [13,17].

(d) Accumulative roll bonding (ARB)

ARB process utilizes traditional rolling resource. In ARB, specimen in a form of sheet is rolled to half of its thickness, then rolled specimen is slice into two pieces and both the sliced sheets are stacked together, so that the original thickness of sheet specimen are restored. Prior to rolling again, the stacked sheet contact surfaces are wire brushed and degreased, to attain good bonding between the sheets, the sheet then rolled again to half of its thickness. The cycle of rolling, cutting, brushing and

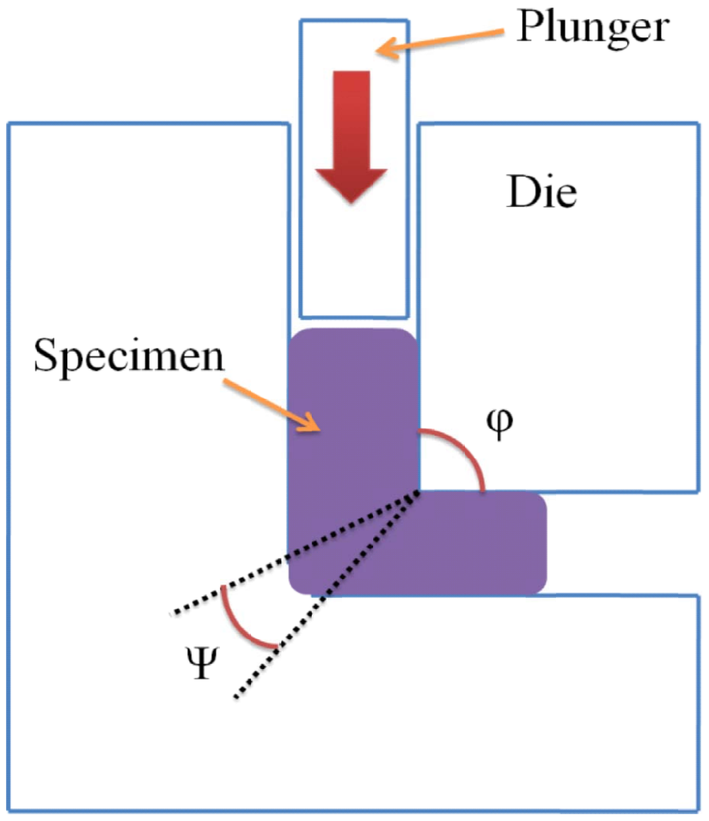

Fig. 2. Schematic representation of ECAP principle, adapted from [74].

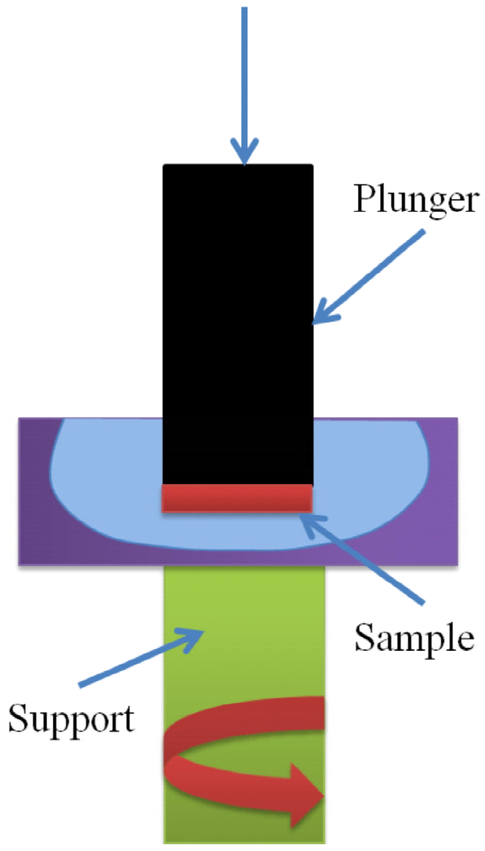

Fig. 3 Schematic representation of HPT principle, adapted from [8].

stacking processes continuous till the large accumulation of strain takes place in the sheet specimen. The schematic of the process is shown in Fig. 4. The ARB process results pancake like microstructural configuration which is stretched in lateral direction and not equiaxed along three dimensions, similar to the microstructure obtained during traditional rolling process [18,19].

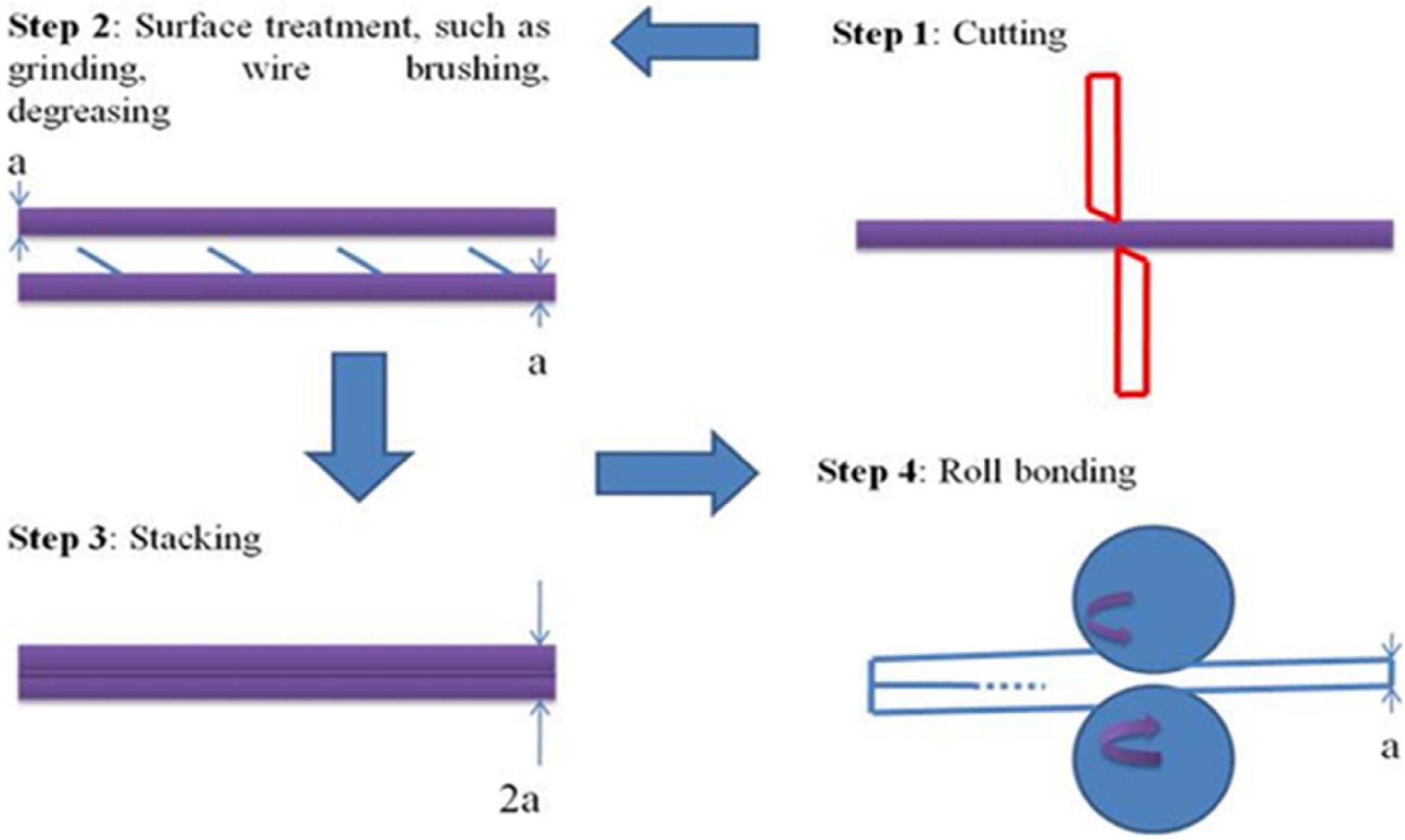

Fig. 4. Schematic representation of ARB principle, adapted from [18].

(e) Twist extrusion (TE)

TE is another type of SPD process, in which simple shear deformation takes place [13]. In this process, a specimen is drive through an extrusion die. The specimen maintains its size and shape during twisting at desired angle about its longitudinal axis due to which the specimen regains its size and shape after every TE pass and results grain refinement. The repetition of the process results worthy grain refinement. The variety of shapes can be handled by this process except of circular shapes. This process results inhomogeneous deformation, which is smallest near the axis of extrusion [4]. The schematic representation of TE process is shown in Fig. 5.

ECAP and HPT techniques of SPD is used for the first job to fabricate nanostructured alloys and metals deformed up to the nano range [20,21]. All the above listed basic SPD processes are becoming accepted, because of its capability to achieve substantial grain refinement in bulk materials. Among all the major SPD processes our present review is focussed on the grain refinement through MDF process of various materials. The changes in various properties of the materials during MDF process along with various parameters such as processing conditions, strain applied, grain refinement is also considered in the current study. The introduction section defines about basic SPD techniques, next section explains different studies on MDF of different materials and there assessment, pre final section reports tabular plotting of various results and final section concludes the review of various studies on MDF and there constructiveness.

2. MDF PROCESSING OF VARIOUS MATERIALS

The main objective of almost all MDF processing of different materials at various conditions is intense grain refinement and strengthening of the processed materials. Various different mechanisms are defined in various studies behind changes in material properties with the grain refinement.

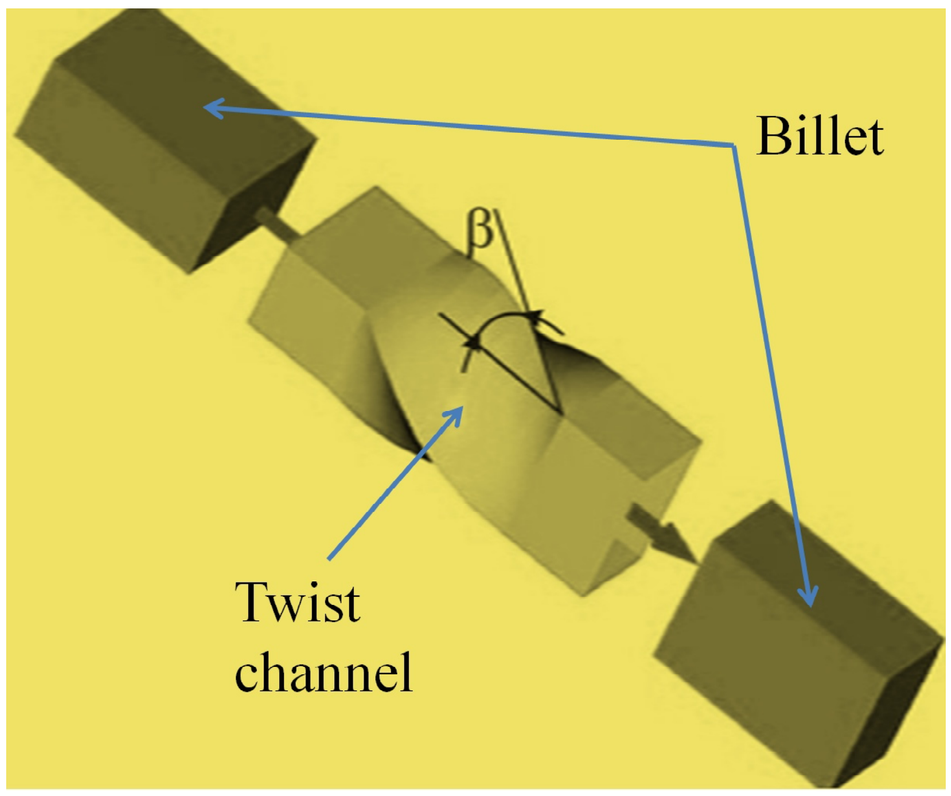

Fig. 5. Schematic of TE processing, adapted from [75].

2.1. MDF processing of Cu and Cu alloy

The pure copper and aluminum alloy are processed at low and high temperatures during MDF. The micro-shear/kink bands developed and subgrains with high angle grain boundaries are formed during MDF and results new refined grain structure. The grain refinement at low temperature results due to the dynamic structuring of high angle grain boundaries at lower strain and at high temperature, the high frequency of dynamic recovery at large strain results grain refinement [14]. In another study of multiple compressions in a channel die (MDF) of copper at 298K and 418K, the imparted equivalent strains of 4 and 8 results enhanced flow stress and strain rate sensitivity of copper [22].

The MDF under plain strain conditions applied at a steady strain rate of 0.001/s to copper and two phases Al-Cu alloy results extreme grain refinement along with improved hardness and flow stress. The Cu is deformed up to cumulative equivalent true strain of 7, results improved strength from 470 MPa to 640 MPa with crystalline size of 21.84 nm, while for Al-Cu is deformed to the cumulative equivalent true strain of 1.5 and strength is improved from 320 MPa to 375 MPa with 20-25 μm grain size. In two phase Al-Cu alloy, shear band formed during MDF is found as the failure mechanism [23]. The high leaded tin bronze (copper alloy) is deformed through MDF up to the equivalent strain of 0.75 at room temperature (RT). The homogeneity along with improved hardness and strength is achieved. The decreased crystallite size from 240 nm to 90 nm along with increased dislocation density to 1.52 x 10^{15} /m^2 is reported as main reason for improved strength from 80 MPa to 185 MPa and hardness from 75 Hv to 175 Hv after 0.75 MDF strain [24].

MDF is used to prestrain copper to study the creep resistance and strain rate sensitivity of flow stress at elevated temperature of 373K during creep as a function of prestrain. During creep deformation the prestrain material results deformation resistance at elevated temperature, the deformation resistance is decreased and strain rate sensitivity of the copper is increased with the pre-deformation increases [25], while the MDF and twist extrusion of oxygen free copper is produced UFG structure to study the thermal stability at both high and room temperature. The results of microstructural studies is found more stable of MDF or twist extrusion processed Cu, as compare to ECAP of HPT processed Cu. Among the various SPD processes, the MDF processed Cu reports better thermal stability for the similar grain size deformed copper, which is correlated in terms of decreased crystallite size and dislocation density [26]. In different study of Cu processed by MDF the isothermal annealing behaviour is studied at 503-573K after straining up to 6.0 [27].

2.1.1. Appraisal of MDF processing of Cu and Cu alloy:

(i) In terms of deformation mechanism and microstructural transformation.

For the MDF of pure copper, the microstructural change is observed as identification of many mutually crossing micro-shear bands/kind bands at different directions which is due to application of strain by changing the loading directions. With repeating MDF, the high angle grain boundaries are resulted and dynamic grain growth is also resulted due to continuous dynamic recrystallization. The fragmentation of grains due to induced strain developed new grains structure and the continuous dynamic recrystallization formed the restoring mechanism for dynamic recovery during MDF [14]. The higher misorientations between grains resulted higher angle grain boundaries of copper during MDF which was due to higher strain rate sensitivity [22]. Initially strain hardening and later on grain refinement strengthen the copper during MDF [23]. Moreover, the MDF strengthening of high leaded tin bronze (copper alloy) involves formation of sub-grains within twin lamellae, construction of twins and increased dislocation density [24]. The higher fraction of high angle grain boundaries increased the dislocation eradication rate from the crystal of copper and deformation resistance of predeformed Cu at elevated temperature is decreased with strain rate sensitivity of increased flow stress and increased predeformation [25]. The discontinuous and continuous static recrystallization of copper during MDF results different dislocation behaviour (heterogeneous and homogeneous) with different grain sizes. The incubation stage for fresh grain formation, recrystallization process and normal grain development are reported for different strain applications [27].

The microstructural refinement of Cu and its alloy results majority of crystallite size fall within a range of 21-378 nm with the applied strain $\leq$18 can be seen in Fig. 6 and Table 1. Some work report quite higher crystallite size <1000 nm with applied MDF stain of 6 [27] and in the range of 225 nm, but after very high MDF strain of 50 [26]. This could be due to the different deformation behaviour of Cu alloy and its processing conditions. The MDF process is constructive towards the fabrication of crys-

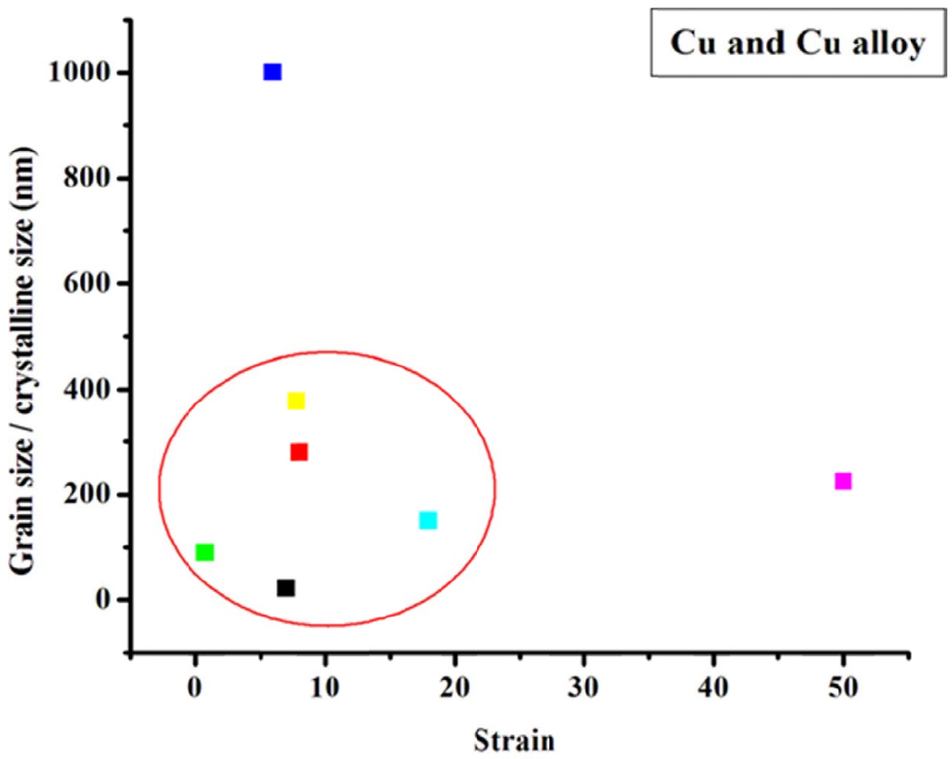

Fig. 6. Grain size / crystalline size vs. strain plot for Cu and Cu alloy.

tallite structure up to 21 nm for copper [23] and as discussed above the micro-shear bands, higher angle grain boundaries, strain hardening, twin lamellae, construction of twins and increased dislocation density along with MDF straining forms the strengthening mechanism for Cu and its alloy.

2.2 MDF processing of Mg alloy

The MDF is successfully applied on AZ61 Mg alloy at room temperature with small pass strain of 0.1 up to the cumulative strains of 2.5. The ageing heat treatment is also applied before and during MDF. Mechanical twinning is the major mechanism behind strengthening of the alloy with 1 μm spacing and 0.6 μm decreased grain size. The Mg alloy reports a fine balance of yield strength-500 MPa, ultimate tensile strength-540 MPa and plastic strain to fracture of 4%. The changes in microstructure and mechanical properties is also studied by applying ageing before or during MDF process in Mg alloy [28]. The MDF is also applied to AZ61 Mg alloy at different temperatures of 380 °C, 350 °C, 325 °C, 300 °C, 280 °C, and 250 °C. The equivalent strain up to 4.158 resulted 8 mm refined grain with improved mechanical properties. The dynamic recrystallization is the main mechanism behind fragmentation of grains during MDF [29].

In a different study during MDF of AZ61 Mg alloy, the cumulative strain of 4 at a true strain rate of 3 x 10^{-3} s^{-1} is applied in decreasing temperature range within 623K to 503K results average grain size of 0.8 mm. The fabrication of ultrafine grained structure is resulted due to the combined mechanism of continuous dynamic recrystallization, mechanical twinning and kinking. The ultimate tensile strength - 440 MPa, with 20% ductility at room temperature is achieved during MDF. The superior formability is found in UFG AZ61 Mg alloy makes it to further deform by cold rolling with ageing process, which further raised the strength of the alloy to 550 MPa without loss of much ductility and limits to 14% [30], in a similar work, on the same alloy with decreasing temperature range from 643K to 483K, the grains are refined to less than 1 μm average size with 99 Hv hardness and 20% cold formability is achieved through MDF, which is further deformed by cold rolling process, and 120 Hv hardness is achieved [31]. Moreover, AZ61 Mg alloy is also deformed at room temperature up to cumulative strain of 2 by passing small strains per pass of 0.1. During MDF, the coarse grains are fragmented into finer size by mechanical twinning process results twins with spacing less than 1 μm, yield strength of 480 MPa, tensile strength of 525 MPa along with 5% ductility [32].

Mg-Gd-Zn alloy is deformed by applying hot rolling, MDF and annealing heat treatment processes to study the effect of texture and grain size on ductility and tensile behavior at room temperature. The grain size is negligibly effect room temperature ductility of the alloy, as the twinning is introduced during post deformation leads to premature failure and small post-uniform elongation [33]. The cumulative strain of 1.5 is applied during MDF at room temperature of AZ21 Mg alloy followed by various annealing treatments. The UFG AZ21 is fabricated during cold MDF with increased tensile strength and small ductility loss. The grain orientation introduced during mechanical twinning by MDF is responsible for changes in property of the alloy. The annealing effect microstructure evolves during heat treatments. The homogenous structure with 3.8 mm mean grain size is obtained, which is weak as compared to the as-annealed specimen and results significant increases in ductility and stretch formability [34]. A further annealing behavior of Mg alloy AZ31 under isothermal condition deformed through MDF at ambient temperature up to 1.5 cumulative strains is reported at 473K. The high density refined twins distributed homogenously over the volume is reported during MDF strain application. The high strain concentration is build up at the intersection point of twins and grain boundaries. The site for nucleation of recrystallization is resulted due to the development of more types of twins and their intersections. During this study, MDF is established as successful method for the formation of finer twins with high density homogenously [35], in a similar material study, the isothermal behaviour is investigated at a temperature scale of 443K to 518K and 623K to

423K and improved mechanical properties are reported in different studies [36,37], a better homogeneity is also reported in recent study through MDF [24]. In the study of AZ31 microstructures build up during MDF followed by annealing. The cumulative stain up to 5 is applied, decreased the grain size evolved during annealing to 1 μm. The change in loading direction during MDF introduced various intersecting deformation twin at high density and results homogenous microstructure [38].

The hot MDF is employed to refine grain in as-cast AZ80 Mg alloy. The applied strain in the scale of 2-2.4 results homogeneous microstructure with fine energetic recrystallized grains. The main cause for grain fragmentation is the formation of micro-bands in various directions, which intersect each other and results continuous disintegration of coarse grains. In overall the grain refinement during is resulted due to continuous dynamic recrystallization [39]. The decreasing temperature condition is applied from pass to pass within 623K to 403K to carry out MDF up to the cumulative strains of 5.6 of AZ31 Mg alloy. The grain size of 0.23 μm is fabricated during MDF which is resulted due to continuous dynamic recrystallization at final deforming temperature of 403K. The superior yield strength-526 MPa with moderate ductility-13% is resulted during MDF of AZ31 Mg alloy at room temperature [40]. The changed process temperature from 623K to 423K pass to pass upto cumulative strains of around 5 during MDF of AZ31 Mg alloy results 0.36 mm grain size at final deforming temperature of 423K. The kinks band developed in various loading direction during MDF refines the grain structure [41].

In one of the different study, a particulate reinforced magnesium matrix composite is practiced using stir casting deformed through MDF under 370 °C to 450 °C results improved yield strength (Y.S) and ultimate tensile strength (UTS) of the composite [42], a relatively similar study but different processing temperature of 420 °C results uniform particle distribution along with enhanced mechanical properties [43]. The ZK60 Mg alloy, mechanical properties are improved by using MDF process and partial remelting route. The effect of holding time and remelting temperature on microstructure is also studied. The raise in thixoforming temperature between 560 °C to 574 °C resulted improved tensile strength of the alloy from 290 MPa to 315 MPa [44].

2.2.1. Appraisal of MDF processing of Mg alloy

(i) In terms of deformation mechanism and microstructural transformation

The MDF of Mg AZ61 alloy fabricates ultrafine grains by mechanical twinning, which is resulted due to the random orientation of grains and allows MDF to apply at higher strain and ambient temperature [28,32]. The collective mechanism of kinking, mechanical twinning and continuous dynamic recrystallization is also reported as deformation characteristics for grain refinement during MDF of AZ61 Mg alloy [30,31] along with dynamic recrystallization as well [29]. The mechanism of AZ31 Mg alloy is quite similar to AZ61 Mg alloy. The strengthening of AZ31 Mg alloy is due to the increase in dislocations density, twins formations, twin intersection, kink band formations, and continuous dynamic recrystallization as well for different condition MDF processing of the same alloy [35,37,38,40,41]. The grain boundary sliding and grain orientations controls the MDF deformation of AZ31 Mg alloy under decreasing temperature conditions [36]. In different study of MDF of Mg alloy, twinning forms the strengthening mechanism for Mg-Gd-Zn and AZ21 alloy [33,34]. The grain fragmentation in AZ80 Mg alloy during MDF is resulted due to the development of microbands in various directions intersects each other and also by deformation induced continuous reaction [39]. For AZ91 Mg alloy, dynamic recrystallization along with increased dislocation density refines the grain structure during MDF [42,43].

The grain refinement of Mg AZ31 alloy is reached to the minimum of 0.23 μm after 5.6 MDF strain [40] and 0.36 mm after 4.8 and 5 MDF strains [36,41] compared to other MDF Mg alloy. The majority of the refined grain size after MDF is fall in the range of ≤1 μm of different Mg alloys after different MDF straining can be seen in Fig. 7 and Table 1. Some works on the MDF of Mg alloy reports comparatively higher grain size [33,37], which is due to different deformation characteristics of different Mg alloy and processing conditions. The mechanical twinning, kinking, grain orientation, continuous dynamic recrystallization, twin intersection, development of microbands, increased dislocation density are characterize as main deformation mechanism for different Mg alloys as discussed earlier.

2.3. MDF processing of Al and Al alloy

Al 6061 alloy is processed by MDF and aging treatment to fabricate UFG structure with tensile strength of 385.7 MPa and ductility of 11.17%. The separated ultrafine precipitate particles surrounded by the grains, increased dislocation density, and reduced grain size improve the strength of the alloy and residual stress relieve during aging improves

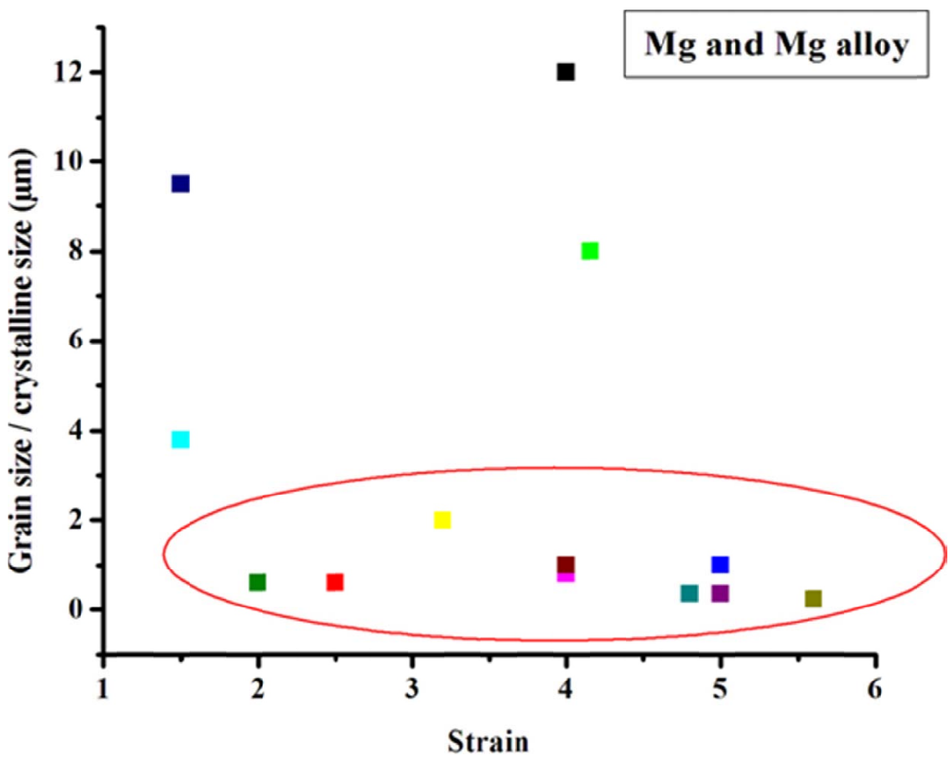

Fig. 7. Grain size / crystalline size vs. strain plot for Mg and Mg alloy.

the ductility of the alloy. The mass of the UF (ultrafine) particles are distributed and surrounded by the grains after aging helps in dislocation accumulation, increases dislocations storage ability and resist dislocation slip [45]. The Al 6061 alloy is also processed by MDF at liquid nitrogen temperature up to the cumulative strain of 5.4 results equiaxed sub-grain microstructure of 250 nm average sizes. The hardness of the Al alloy is reached to 115 Hv along with 388 MPa, ultimate tensile strength, and 4.5% ductility. The occurrence of high dislocation density is featured to the creation of equiaxed sub-grain structures [46]. The hot MDF is introduced during the grain refinement of coarse grained Al-7475 alloy at 490 ^{0}C under a strain rate of 3 x 10^{-4} s^{-1}. The grain refinement is resulted due to the regular advancement of micro-shear bands in different directions, with increased numbers and misorientations [47]. In other study on Al-7475, the effect of strain rate and its discontinuous alteration on the microstructural and deformation behaviour are studied during MDF at 763K. The discontinuous strain rate results differently due to the rate of application. The grain refinement at lower strain rate of 3 x 10^{-2} s^{-1} is controlled by grain boundary sliding and results homogenous refinement, but at higher strain rate of 3 x 10^{-4} s^{-1}, the grain refinement takes place only close to the original grain boundaries with partial grain refinement directed by homogeneous dislocation movements [48].

The effect of temperatures from 573K to 763K during grain refinement of Al-7475 alloy through MDF is studied. The fine-grained structure is build up mainly by the structuring of micro-shear bands, which is followed by boundary misorientations and increase in numbers. With the increase in temperature of processing, the plastic flow mechanism of the alloy changes and controlled primarily through grain boundary slidings. The temperature in between 573K to 763K develops the original grains at a new colony. The further high strain rate during MDF leads to non homogenous deformation via formation of micro-shear bands crossing in novel grain interiors and accelerate the kinetic of grain fragmentations [49].

Aluminum alloy AA 3104 is deformed up to strain of 3.56 by MDF results increased flow stress with strain. The large range of shear bands with higher misorientations are also resulted while the microstructure deformed up to 0.86 strains results extended boundaries and dislocation cells [50]. A three dimensional dislocation density based two-phase composite model is used during the MDF of aluminum AA1100 alloy. A simulation and experimental studies are performed and compared, which forms the good agreement with each other in terms of yield strength and average grain size. The study prove that three dimensional dislocation density based two-phase composite model can sensibly be applied to predict average grain sizes and yield strength of the material before practically applying MDF [51]. The Al-3Mg-Sc(Zr) alloy is MDF up to the strain of 3 in the temperature range of 20-400 °C. At room temperature, considerable grain refinement fabricates the weak textures and substructure refinement while at 300 °C and above to it, MDF results homogenous intra-granular rotations and deformations forms stronger texture and novel microstructures [52]. The MDF of rheoforged aluminum alloy A356 is applied to study the microstructure and mechanical properties changes in globular and dendritic states. The optimal globular structure under three MDF pass of rheoforged specimen is imposed successfully as compared to the dendritic one. The improved strength and hardness owing to the breaking of Si particles and work hardening of primary Al phase is achieved [53]. In the latest study, hot-extruded AA5056-H38 aluminum alloy is MDF with non isothermal annealing. The effect of applied strain post annealing combination on the mechanical properties, microstructural evolved, and electrical conductivity is examined [54]. In a different report of MDF of Al-Mg alloy, the dislocation emission from sub-grain boundaries with 100 nm sub-grained structure is studied. This study defines the presence of dislocation density in sub-grained structures considerably belongs to partial dislocation emission [55]. The Al-4wt.%Cu, binary alloy is used to distinguish the processing by MDF and HPT. The processing of alloy through HPT

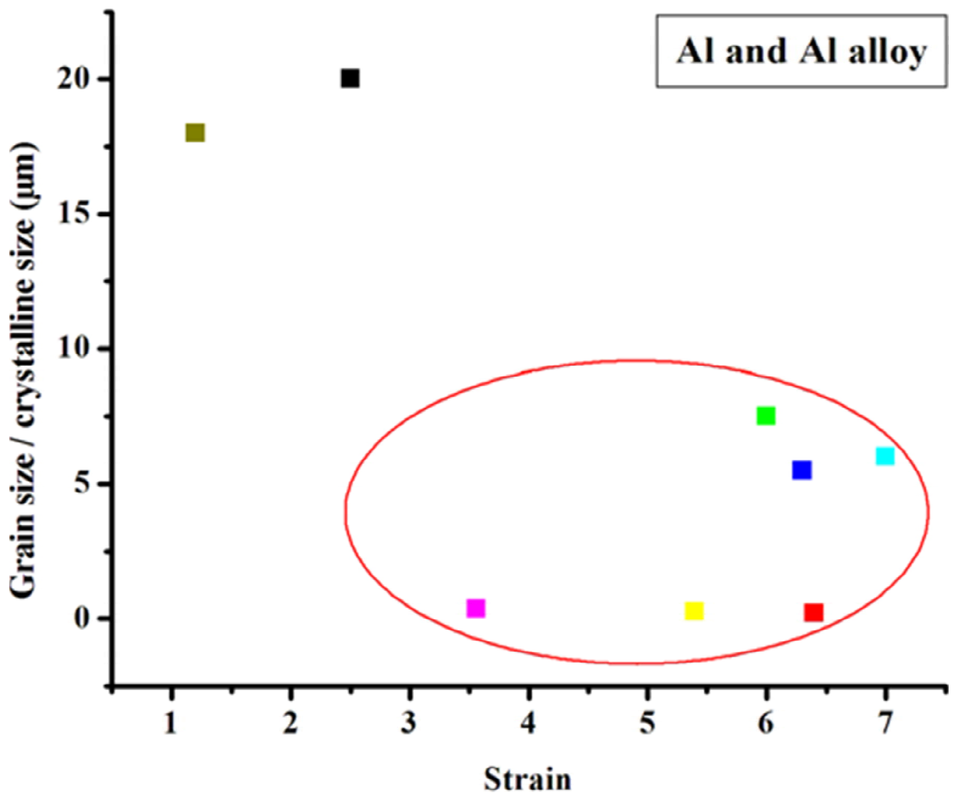

Fig. 8. Grain size / crystalline size vs. strain plot for Al and Al alloy.

results higher homogeneity and hardness along with equilibrium grain size structures [56].

2.3.1. Appraisal of MDF processing of Al and Al alloy

(i) In terms of deformation mechanism and microstructural transformation

The MDF strengthening of Al-Cu alloy is resulted mainly by work hardening, not by grain refinement during MDF. The fragmentation of eutectic mixture and localized shear band formation in the soft Al matrix not allows severe deformation due to formation of cracks at lower true strain [23], while in other study, the shear band formation is outline as the strengthening mechanism for Al-4wt.%Cu [56]. The strengthening of 6061 Al alloy during MDF is due to increased dislocation density and dispersion of ultrafine precipitate constituents within a grains after aging treatment [45] while for same alloy, along with increased dislocation density, deformation bands strengthens the alloy [46]. The MDF of 7475 Al alloy is resulted due to microshear bands development with increased numbers and misorientations in various directions and by grain boundary sliding, mechanism similar to continuous dynamic recrystallization [47-49]. The AA 3104 Al alloy also deformed (MDF) under the common mechanism of shear band formation and higher misorientations process [50], on the other hand, the work hardening of α-Al and Si particle breakdown forms the strengthening mechanism for A356 Al alloy [53]. The Al-3Mg-Sc alloy strengthen by grain fragmentation during MDF, results due to intragranular deformation and orientation of grains [52]. In the MDF of AA5056-H38 Al alloy, the sectioning of primary coarse intermetallic particles into ultrafine dispersoids redistributes them in matrix and formation of lamellar structure strengthen the alloy [54].

The grain sectioning during MDF is reached to minimum of 0.20 μm for AA1100 Al alloy [51] and 0.25 μm for 6061 Al alloy as well [46]. The majority of refined grain structure through MDF falls in the scale of 0.20 μm to 7.5 μm of different Al alloys can be seen in Fig. 8 and Table 1. Some MDF processing of Al alloy reports comparatively higher grain size [23,54], which is highly depend upon behaviour of Al alloy and processing conditions. The common strengthening behaviour for Al alloy are work hardening, shear band/ microshear bands formation, increased dislocation density, grain boundary sliding, and higher misorientations of grains as discussed above.

2.4. MDF processing of steels

The austenitic stainless steel (SUS 316) is deformed upon MDF at the temperatures of 77K and 300K. The grain refinement at 77K is more significant than at 300K during MDF. The grain size of 5-10 nm is obtained along with 2.1 GPa tensile strength and 20% elongation after the cumulative strain application of 6 at 77K. The grains fragmentation is achieved through mechanical twinning and martensitic transformation results mechanical twins with 10-300 nm spacing [57]. In another study, austenitic steel of 304 type is deformed upon warm MDF at 500 °C and 800 °C. The two different temperatures result different mechanism of grain refinement during warm MDF. The MDF at 500 °C results development of 0.22 μm and at 800 °C results development of 0.69 μm average grain size. The processing at 500 °C results almost same fraction of low and high angle grain boundaries while processing at 800 °C results 0.45 and 0.55 fractions, low and high angle grain boundaries. At 500 °C MDF, continuous dynamic recrystallization is resulted common strain induced boundaries, on the other hand, discontinuous recrystallization at 500 °C results migration of grain boundaries which leads to the creation of annealing twins [58]. The low carbon steel is MDF at room temperature followed by post annealing deformation at 500 °C for 60 seconds results ferrite grains refinement upto 1.2 μm sizes with accumulative strain of 2.8. The ultimate tensile strength of 1043 MPa, with 8.8% elongation is reported, the static recrystallization is identified as grain refinement mechanism at 500 °C. During microstructural evolution the new grains are formed by nucleation of fresh grain within deformed grains [59]. The very high strain is

imparted in cast iron aluminide with coarser borides distributions at high temperature through MDF. The deformation results fine dispersion of boride particles with sound ductility at room temperature along with exceptional creep strength up to the temperature greater than 700 °C [60]. The high strength low alloy (HSLA) steels is deformed through MDF and inter critical annealing methods using thermo mechanical and thermal processing, to study slurry and cavitations erosion. The dual phase (DP) ferrite–martensite is reported to have 1.5 times better erosion resistant microstructure then compared to as received HSLA steel. The elevated hardness, toughness, and superior strain hardening ability of DP-HSLA steel compared to as received and MDF HSLA steels is featured to result superior erosion resistant [61]. In another study of warm MDF of AISI 1016 steel results finer substructure with the increase of MDF strain. The microstructure of the steel reports pearlitic-cementite sectioned into ultrafine units of around 100–300 nm size. During MDF, crystallographic slip, grain boundary sliding, and random grain rotation is the principal mode of deformation and grain refinement and recovery for ferrite. The MDF process results average grain size of about 0.6 μm with 0.7 fractions of high angle grain boundaries. The ultimate tensile strength of steel is increased to about 100% along with retained ductility of 10% [62]. The warm MDF of HSLA leads to produce average grain size of 0.6 μm along with improved ultimate tensile strength of 813 MPa, with 12.5% ductility [63]. The plain low carbon steel is MDF at 500 °C results improved tensile strength of 791 MPa and hardness of 253 VHN of the steel. The average grain size of 0.5 μm is evolved during MDF with high angle grain boundaries of 0.81 fractions [64]. The Fe–32%Ni alloy is deformed upon MDF at the temperatures of 773K and 1073K and strain rate of 10^{-2} s^{-1}. The MDF of the steel results improved strength and refined grain structures. At the temperature of 1073K, the grain refinement system is categorize as discontinuous dynamic recrystallization while at 773K, the mechanism of grain refinement is discontinuous dynamic recrystallization [65]. The ultrafine grained 316 L stainless steel is obtained by processing through warm MDF at 600 °C up to 2.8 equivalent strains, results 0.86 μm average grain size, 300 VHN hardness, and also improves sliding wear and pitting corrosion resistance of the steel [66].

In the study of dry sliding wear performance of the mild steel processed by MDF up to nine pass fabricates ferrite grains of average size 0.5 μm. The different loading direction during MDF results sectioning of pearlitic cementite to about 200 nm particles size, which is not contributed to enhance the wear resistance of the mild steel [67]. In another study, about change in mechanical and wear behaviour of AISI 1024 steel after warm MDF at 500 °C, the cementite particle is fragmented into submicron sized results improved strength and hardness properties significantly along with decreased total % elongation values. The dry sliding wear resistance of the steel alloy is not improved with submicron sized microstructures [68].

The AISI201 stainless steel is MDF at 973K in air fragmented initial grains of 35 mm into 5 μm size. The dynamic recovery and continuous dynamic recrystallization phenomenon are accountable for the arrangement of fine austenitic grains during strain induction [69]. The MDF of 304H austenitic stainless steel is reported in the temperature range between 500 °C to 700 °C. The formation of ultrafine grain structure is accompanied by dynamic recrystallization along with MDF reduced the grain size from 0.3 μm to 0.1 μm during decreasing temperature from 700 °C to 500 °C [70].

2.4.1. Appraisal of MDF processing of steels

(i) In terms of deformation mechanism and microstructural transformation

The mechanical twinning with lamellar arrangement of twins along with martensitic transformation forms the strengthening mechanism through MDF grain refinement of austenitic stainless steel (SUS 316) [57] while for 316L austenitic stainless steel the combination of strain hardening and Hall–Petch strengthening is the mechanism [66]. For 304 austenitic stainless steel, continuous dynamic recrystallization with low and high angle boundaries is the major characteristics of alloy strengthening [58] and static recrystallization for grain refinement of low carbon steel during MDF [59]. The MDF of iron aluminide alloy strengthen its creep resistance through elongated boride particles distributions [60]. The refinement of ferrite–pearlite and development of dual-phase ferrite–martensite microstructure in HSLA steel during MDF strengthen the alloy [61]. In the MDF of AISI 1016 steel, the ferrite grain is refined through crystallographic slip; grain subdivision and recovery upto certain strain level, but at higher strain random grain rotation and grain boundary sliding forms the major strengthening mechanism [62], also for MDF of HSLA steel [63]. The formation of high angle grain boundaries with misorientation distribution strengthen the plain low

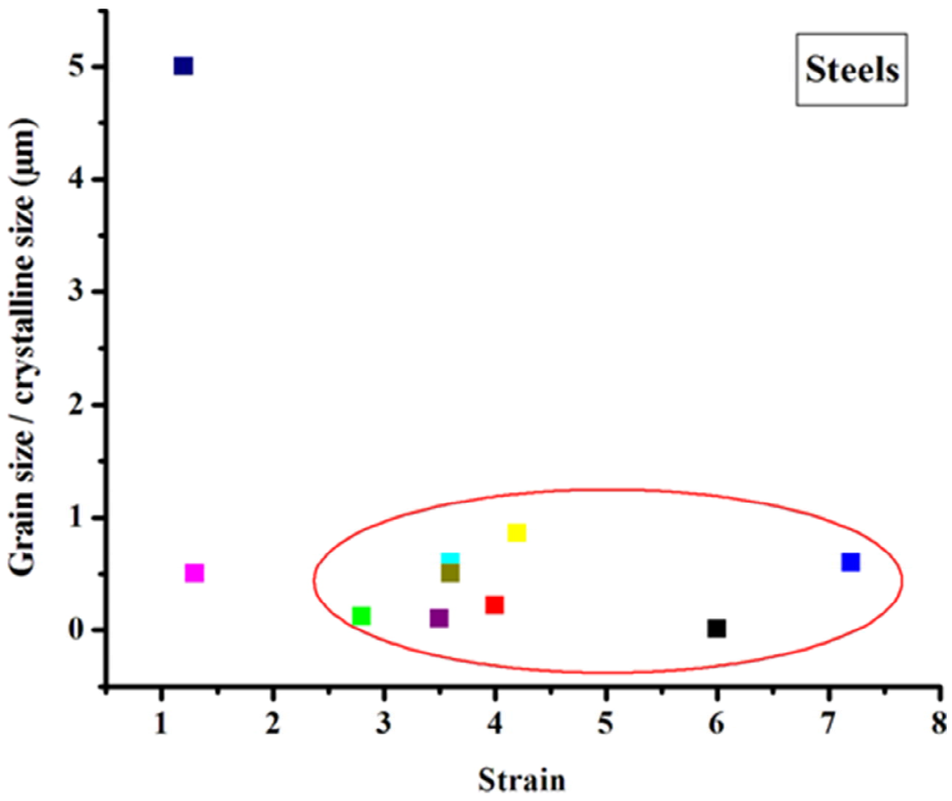

Fig. 9. Grain size / crystalline size vs. strain plot for steels.

carbon steel through MDF [64]. The misorientations of subgrain boundaries increase by common intrinsic slip and the inclusion of accommodated dislocations holds novel ultra-fine grains formation. The continuous dynamic recrystallization forms the grain refinement mechanism for Fe–32%Ni alloy [65] along with it discontinuous dynamic recrystallization also played the role during MDF of S304H austenitic stainless [70]. The absorption of dislocations through grain boundaries and higher misorientations between the finer grains strengthens AISI 1024 steel via MDF [68]. The intersecting microbands, increased grain misorientations, along with high angle grain boundaries is characterized to continuous dynamic recrystallization and dynamic recovery are accountable for the creation of MDF strain-induced fine austenitic grains in AISI201 stainless steel [69].

The minimum grain size of 10 nm is resulted during the MDF of SUS 316 austenitic stainless steel [57], while the region of maximum refinement achieved falls in the scale of 0.01-0.86 μm can be seen in Fig. 9 and Table 1. The AISI201 stainless steel shows quite high, 5 μm grain sizes with 1.2 strains [69] on the other hand, quite low 0.5 μm grain size through 1.3 strains is also obtained during MDF of plain low carbon steel [64]. The different mechanism of steel as well as deformation situations may be the reason behind differences. The intersecting microbands, increased grain misorientations, high angle grain boundaries, static recrystallization, continuous and discontinuous dynamic recrystallization and dynamic recovery are the major strengthening mechanism of different steels via MDF processing.

2.5. MDF processing of Ti alloy

A plain-strain cryogenic MDF is developed to refine the microstructure of commercial purity titanium of grade 2. During MDF, the specimens and plunger are immersed within a liquid nitrogen bath and the temperature near to -190 °C is maintained. The microstructural refinement takes place due to the formation of twins and slip bands increased the energy stored in an alloy and also provides sites for nucleation. The microstructure refinement to the scale of 100-200 nm is achieved with small deformation stain of 1.18, with improved room temperature yield strength of 840 MPa and elongation to failure of 12%. In the same work uniform microstructure is also achieved by low temperature recrystallization annealing along with a good combination of yield strength of 570 MPa and elongation to failure of 31% [71]. In another work on beta Ti alloy (Ti + 25 mol.%(Ta,Nb,V) + (Zr,Hr,O)) is targeted, to develop the new mechanical properties in a alloy through cold SPD via MDF and cold rolling along with its effect on microstructure and elastic modulus is experimented. The MDF and cold rolled sheet results lower elastic modulus than only cold rolled sheet with isotropic elastic modulus and around ~1 μm grain size is obtained after plain rolling of sheet. The MDF and plain rolling of the alloy at room temperature successfully evolved low elastic modulus of 60-65 GPa, strength of 1100 MPa, and ductility of greater than 10% [72]. In different study related to MDF of Ti, microstructural evolution under controlled dynamic loads in an adiabatic shear band is studied. In the core of shear band microstructure consist of equiaxed grains of 0.05-0.08 μm in diameter [73].

3. TABULAR COMPARISON OF VARIOUS LITERATURES

The detailed study of literatures is given in earlier section 2. This section helps in observing of changing properties of different metals and alloys during MDF in terms of processing conditions, materials used, strain applied, final grain size achieved, and properties achieved during MDF is shown in Table 1.

4. CONCLUSION

There are many researches on various materials processed by MDF and various different studies are reported to study the effect of MDF on the material properties. The present review covers and reports

about many of the different studies on MDF and tried to cover as much as possible. The MDF process is an emerging procedure of SPD to vary the functional applications of the materials. The MDF of Cu, Al, Mg, steels, and other alloys are found to be interests of studies along with other materials. The comparative studies describes different materials deformation scale in terms of different MDF processing, and strain applied, which may help in selection of various materials accordingly to required properties for different applications. The continuous/discontinuous dynamic recrystallization, increased dislocation density, shear band formation and there intersection, grain orientation with high angle grain boundaries, twin formation, and stain hardening are the major strengthening mechanism during MDF of different material. Various studies prove that MDF is an effective process to vary the material strength and other properties, by refining the microstructure up to nano scales. The advantages of MDF process is also enumerated in the earlier section. The other SPD processes like ECAP, HPT, ARB, are comparatively more developed than MDF and reported in higher fraction, thus MDF route founds as an emerging trend and area, to fabricate novel grain structures and properties up to nanoscale. For the better development of MDF process more number of researches is required to be reported in future under various processing conditions and on different materials. With the current attempts, we are contributing a platform to the researcher by building up a significant base of updates related to MDF processing, materials, and results that lead to an immense choice of alloy, processing conditions and other parameters to select for future studies, by reading and comparing various previously published literatures using present review. The present review in several orders is increasing the knowledge related to MDF and alloys are used to shorten socially necessary complexity to the further research using MDF process.

REFERENCES

[1] P. Bridgman // *Jour. App. Phys.* **14** (1943) 273.
[2] P. Bridgman // *Jour. App. Phy*s. **17** (1946) 692.
[3] R. Z. Valiev // *Nat. mat.* **3** (2004) 511.
[4] R. Z. Valiev and A. A. Nazarov // *Bulk nanostructured mater.* (2009) 21.
[5] A. Azushima, R. Kopp, A. Korhonen, D. Y. Yang, F. Micari, G. D. Lahoti, P. Groche, J. Yanagimoto, N. Tsuji and A. Rosochowski // *CIRP Ann. Manuf. Tech*. **57** (2008) 716.
[6] T. C. Lowe and R. Z. Valiev // *Jom* **56** (2004) 64.
[7] J. Xing, H. Soda, X. Yang, H. Miura and T. Sakai // *Jour. Japan Inst. Light Met.* **54** (2004) 527.
[8] R. Z. Valiev, Y. Estrin, Z. Horita, T. G. Langdon, M. J. Zechetbauer and Y. T. Zhu // *Jom* **58** (2006) 33.
[9] O. Valiakhmetov, R. Galeyev and G. Salishchev // *Phys. met. metall.* **70** (1990) 198.
[10] R. Galeyev, O. Valiakhmetov and G. Salishchev // *Russian Metall*. **4** (1990) 97.
[11] S. Zherebtsov, G. Salishchev, R. Galeyev, O. Valiakhmetov, S. Y. Mironov and S. Semiatin // *Scrip. Mater.* **51** (2004) 1147.
[12] O. Kaibyshev // *Jour. Mater. Proc. Tech.* **117** (2001) 300.
[13] Y. Estrin and A. Vinogradov // *Acta mater.* **61** (2013) 782.
[14] T. Sakai, H. Miura and X. Yang // *Mater. Sci. Eng. A* **499** (2009) 2.
[15] Y. Iwahashi, J. Wang, Z. Horita, M. Nemoto and T. G. Langdon // *Scrip. Mater.* **35** (1996) 143.
[16] R. Z. Valiev and T. G. Langdon // *Prog. Mater. Sci.* **51** (2006) 881.
[17] G. Sakai, K. Nakamura, Z. Horita and T. G. Langdon // *Mater. Sci. Engg. A* **406** (2005) 268.
[18] Y. Saito, H. Utsunomiya, N. Tsuji and T. Sakai // *Acta mater.* **47** (1999) 579.
[19] S. H. Lee, T. Sakai, Y. Saito, H. Utsunomiya and N. Tsuji // *Mater. Trans. JIM* **40** (1999) 1422.
[20] R. Z. Valiev, N. Krasilnikov and N. Tsenev // *Mater. Sci. Eng. A* **137** (1991) 35.
[21] R. Z. Valiev, I. Alexandrov, Y. Zhu and T. C. Lowe // *Jour. Mater. Res.* **17**(2002) 5.
[22] A. Kundu, R. Kapoor, R. Tewari and J. Chakravartty // *Scrip. Mater*. **58** (2008) 235.
[23] A. K. Parimi, P. Robi and S. Dwivedy // *Mater. Des.* **32** (2011) 1948.
[24] R. Gupta, S. Srivastava, N. K. Kumar and S. K. Panthi // *Mater. Sci. Eng. A* **654** (2016) 282.
[25] Y. Li, X. Zeng and W. Blum // *Mater. Sci. Eng. A* **483** (2008) 547.
[26] J. Gubicza, S. Dobatkin, E. Khosravi, A. Kuznetsov and J. Lábár // *Mater. Sci. Eng. A* **528** (2011) 1828.
[27] A. Takayama, H. Miura and T. Sakai // *Mater. Sci. Eng. A* **478** (2008) 221.
[28] H. Miura, T. Maruoka and J. Jonas // *Mater. Sci. Engg. A* **563** (2013) 53.
[29] Q .Chen, D. Shu, C. Hu, Z. Zhao and B. Yuan // *Mater. Sci. Eng. A* **541** (2012) 98.

[30] H. Miura, G. Yu and X. Yang // *Mater. Sci. Eng. A* **528** (2011) 6981.
[31] H. Miura, G. Yu, X. Yang and T. Sakai // *Trans. Nonferr. Met. Soc. Chi.* **20** (2010) 1294.
[32] H. Miura, T. Maruoka, X. Yang and J. Jonas // *Scrip. Mater.* **66** (2012) 49.
[33] D. Wu, R. Chen, W. Tang and E. Han // *Mater. Des*. **41** (2012) 306.
[34] X. Wu, X. Yang, J. Ma, Q. Huo, J. Wang and H. Sun // *Mater. Des.* **43** (2013) 206.
[35] X. Yang, Y. Okabe, H. Miura and T. Sakai // *Mater. Des*. **36** (2012) 626.
[36] X. Y. Yang, Z. Y. Sun, X. Jie, H. Miura and T. Sakai // *Trans. Nonferr. Met. Soc. Chi.* **18** (2008) s200.
[37] X. Yang, Y. Okabe, H. Miura and T. Sakai // *Jour. Mater. Sci.* **47** (2012) 2823.
[38] X. Yang, H. Miura and T. Sakai // *Mater. Des.* **44** (2013) 573.
[39] Q. Guo, H. Yan, Z. Chen and H. Zhang // *Mater. Charac.* **58** (2007) 162.
[40] J. Xing, X. Yang, H. Miura and T. Sakai // *Mater. Trans.* **49** (2008) 69.
[41] J. Xing, H. Soda, X. Yang, H. Miura and T. Sakai // *Mater. Trans*. **46** (2005) 1646.
[42] K. B. Nie, X. H. Wang, X. S. Hu, Y. W. Wu, K. K. Deng, K. Wu and M.Y Zheng // *Mater. Sci. Eng. A* **528** (2011) 7133.
[43] K. B. Nie, K. Wu, X. Wang, K. Deng, Y. Wu and M. Zheng // *Mater. Sci. Eng. A* **527** (2010) 7364.
[44] J. Q. Tao, Y. S. Cheng, S. D. Huang, F. F. Peng, W. X. Yang, M. Q. Lu, Q. M. Zhang and X. Jin // *Trans. Nonferr. Met. Soc. Chi.* **22** (2012) s428.
[45] W. Yan, X. Liu, J. Huang and L. Chen // *Mater. Des.* **49** (2013) 520.
[46] P. N. Rao, D. Singh and R. Jayaganthan // *Mater. Des.* **56** (2014) 97.
[47] O. Sitdikov, T. Sakai, A. Goloborodko and H. Miura // *Scri. mater*. **51** (2004) 175.
[48] T. Sakai, H. Miura, A. Goloborodko and O. Sitdikov // *Acta Mater.* **57** (2009) 153.
[49] O. Sitdikov, T. Sakai, H. Miura and C. Hama // *Mater. Sci. Eng. A* **516** (2009) 180.
[50] W. Liu, M. Chen and H. Yuan // *Mater. Sci. Engg. A* **528** (2011) 5405.
[51] A. R. Bazzaz and S. Ahmadian // *Mater. Des.* **34** (2012) 230.
[52] S. Ringeval, D. Piot, C. Desrayaud and J. Driver // *Acta Mater.* **54** (2006) 3095.
[53] A. Dodangeh, M. Kazeminezhad and H. Aashuri // *Mater. Sci. Eng. A* **558** (2012) 371.
[54] M. R. Jandaghi, H. Pouraliakbar, M. R. Khanzadeh, M. K. G. Shiran, G. Khalaj and M. Shirazi // *Mater. Sci. Eng. A* **657** (2016) 431.
[55] X. Yang, S. Ni and M. Song // *Mater. Sci. Eng. A* **641** (2015) 189.
[56] X. Xu, Q. Zhang, N. Hu, Y. Huang and T. G. Langdon // *Mater. Sci. Eng. A* **588** (2013) 280.
[57] Y. Nakao and H. Miura // *Mater. Sci. Eng. A* **528** (2011) 1310.
[58] M. Tikhonova, R. Kaibyshev, X. Fang, W. Wang and A. Belyakov // *Mater. Charac.* **70** (2012) 14.
[59] V. Soleymani and B. Eghbali // *Jour. Iron Steel Res. Inter.* **19** (2012) 74.
[60] D. G. Morris and M. M. Morris // *Acta Mater.* **58** (2010) 6080.
[61] N. Agarwal, G. P. Chaudhari and S. K. Nath // *Trib. Inter.* **70** (2014) 18.
[62] A. K. Padap, G. P. Chaudhari, V. Pancholi and S. K. Nath // *Mater. Des.* **31** (2010) 3816.
[63] A. K. Padap, G. P. Chaudhari, V. Pancholi and S. K. Nath // *Jour. Mater. Sci*. **47** (2012) 7894.
[64] A. K. Padap, G. P. Chaudhari, S. K. Nath and V. Pancholi // *Mater. Sci. Eng. A* **527** (2009) 110.
[65] B. Han and Z. Xu // *Jour. All. Comp*. **457** (2008) 279.
[66] S. V. Muley, A. N. Vidvans, G. P. Chaudhari and S. Udainiya // *Acta Biomater*. **30** (2016) 408.
[67] A. K. Padap, G. P. Chaudhari and S. K. Nath // *Chem. Sust. Dev*. (2012) 219.
[68] A. K. Padap, G. P. Chaudhari and S. K. Nath // *Jour. Mater. Sci.* **45** (2010) 4837.
[69] B. Wang, Z. Liu and J. Li // *Mater. Sci. Eng. A* **568** (2013) 20.
[70] M. Tikhonova, A. Belyakov and R. Kaibyshev // *Mater. Sci. Eng. A* **564** (2013) 413.
[71] D. Hong and S. Hwang // *Mater. Sci. Eng. A* **555** (2012) 106.
[72] A. Danno, C. C. Wong, S. Tong, A. Jarfors, K. Nishino and T. Furuta // *Mater. Des.* **31** (2010) S61.
[73] B. Wang, J. Li, J. Sun, X. Wang and Z. Liu // *Mater. Sci. Eng. A* **612** (2014) 227.
[74] Z. Horita, M. Furukawa, M. Nemoto and T. G Langdon // *Mater. Sci Tech.* **16** (2000) 1239.
[75] V. Varyukhin, Y. Beygelzimer, S. Synkov and D. Orlov // *Mater. Sci. For.* **503-504** (2006) 335.